Lecture Notes in Civil Engineering

Mahdi O. Karkush
Deepankar Choudhury *Editors*

Modern Applications of Geotechnical Engineering and Construction

Geotechnical Engineering and Construction

Springer

Lecture Notes in Civil Engineering

Volume 112

Lecture Notes in Civil Engineering (LNCE) publishes the latest developments in Civil Engineering - quickly, informally and in top quality. Though original research reported in proceedings and post-proceedings represents the core of LNCE, edited volumes of exceptionally high quality and interest may also be considered for publication. Volumes published in LNCE embrace all aspects and subfields of, as well as new challenges in, Civil Engineering. Topics in the series include:

- Construction and Structural Mechanics
- Building Materials
- Concrete, Steel and Timber Structures
- Geotechnical Engineering
- Earthquake Engineering
- Coastal Engineering
- Ocean and Offshore Engineering; Ships and Floating Structures
- Hydraulics, Hydrology and Water Resources Engineering
- Environmental Engineering and Sustainability
- Structural Health and Monitoring
- Surveying and Geographical Information Systems
- Indoor Environments
- Transportation and Traffic
- Risk Analysis
- Safety and Security

To submit a proposal or request further information, please contact the appropriate Springer Editor:

– Mr. Pierpaolo Riva at pierpaolo.riva@springer.com (Europe and Americas);
– Ms. Swati Meherishi at swati.meherishi@springer.com (Asia - except China, and Australia, New Zealand);
– Dr. Mengchu Huang at mengchu.huang@springer.com (China).

All books in the series now indexed by Scopus and EI Compendex database!

More information about this series at http://www.springer.com/series/15087

Mahdi O. Karkush · Deepankar Choudhury
Editors

Modern Applications of Geotechnical Engineering and Construction

Geotechnical Engineering and Construction

Springer

Editors
Mahdi O. Karkush
Department of Civil Engineering
University of Baghdad
Baghdad, Iraq

Deepankar Choudhury
Department of Civil Engineering
Indian Institute of Technology Bombay
Mumbai, Maharashtra, India

ISSN 2366-2557 ISSN 2366-2565 (electronic)
Lecture Notes in Civil Engineering
ISBN 978-981-15-9398-7 ISBN 978-981-15-9399-4 (eBook)
https://doi.org/10.1007/978-981-15-9399-4

This Springer imprint is published by the registered company Springer Nature Singapore Pte Ltd.
The registered company address is: 152 Beach Road, #21-01/04 Gateway East, Singapore 189721, Singapore

Contents

About the Editors

Prof. Mahdi O. Karkush is the President of Iraqi Scientific Society for Soil Mechanics and Foundation Engineering, and Professor of Civil Engineering at the Department of Civil Engineering at the University of Baghdad, Iraq. He received his Ph.D. in Civil Geotechnical Engineering from University of Baghdad, Iraq in 2008. He pursued his B.Sc. in Civil Engineering from University of Babylon, Iraq in 1995 and M.Sc. in Civil Structural Engineering from University of Babylon, Iraq in 1998. Prof. Karkush has authored over 65 technical publications including 50 peer reviewed journal papers. He has supervised over 20 Ph.D. and M.Sc. students. He is a member of the editorial board of several scientific journals. He is a Fellow of The Iraqi Engineers Association (IEA), International Society for Soil Mechanics and Geotechnical Engineering (ISSMGE), UK, and Fulbright scholar, USA.

Prof. Deepankar Choudhury is Institute Chair Professor of Civil Engineering at Indian Institute of Technology Bombay, Mumbai, India and Adjunct Professor ofAcademy of Scientific and Innovative Research (AcSIR) at CSIR laboratories, India. Prof. Choudharyreceived his Ph.D. in Civil Geotechnical Earthquake Engineering from IISc, India in 2002. He served as BOYSCAST Fellow at UC Berkeley USA, Alexander von Humboldt Fellow at TU Darmstadt Germany, JSPS Fellow at Kagoshima University Japan, and as Visiting Fellow/Professor at NUS Singapore, UoW Australia, INU South Korea. Prof. Choudhury has authored over 300 technicalpublications including over 160 peer reviewed journal papers. He has supervised 25 Ph.D. students. He isa Fellow of The National Academy of Sciences, India (FNASc), Fellow of Institutionof Engineers India (FIE), Indian Geotechnical Society (FIGS), Indian Society of Earthquake Technology (FISET). His research contributions in the domain of geotechnical earthquake engineering, foundation engineering and computational geomechanics have been included in several text books, design manual, codes and implemented in field projects.

Evaluating the Performance of Flexible Passive Pile Group in Cohesionless Soil Under the Effect of a Nearby Embankment

Mahdi O. Karkush, Ghofran S. Jaffar, and Omar K. Al-Kubaisi

Abstract Constructing embankments or multi-story structures can induce lateral soil movement especially for cohesionless soil due to its weak structure. In case of having these constructions near an existing pile group, damage can occur to these piles due to the passive loads induced by the soil movement especially when these loads exceed the capacity of the piles. In the current study, the performance of the existing flexible (2 × 1) pile group installed in cohesionless soil has been investigated experimentally under the effect of lateral soil movement induced by a nearby embankment. To simulate the cohesionless soil, a sandy soil having a dry unit weight of 13.5 kN/m^3 has been used in this study. While an aluminum pipe with an outer diameter of 10 mm and a length of 500 mm has been used to simulate the piles. An embedded length (L_e) of 420 mm has been adopted in this study to ensure the flexible behavior for the piles. The embankment loads have been applied at distances of 2.5D, 5D, and 10D from the edge of the pile. The results show that the soil reaction has decreased with increasing the distance between the edge of the piles and the embankment due to the reduction of soil movement pressure. The maximum soil reaction has decreased by (25–33)% in the loaded pile group (LG) and by (50–60)% in the unloaded pile group (UG) with increasing the distance from 2.5D to 10D, respectively.

Keywords Passive pile group · Flexible pile group · Nearby embankment · Cohesionless soil · Experimental study

M. O. Karkush (✉) · G. S. Jaffar
Department of Civil Engineering, University of Baghdad, Baghdad, Iraq
e-mail: mahdi_karkush@coeng.uobaghdad.edu.iq

G. S. Jaffar
e-mail: ghofran_civi@yahoo.com

O. K. Al-Kubaisi
The Faculty of Engineering, The School of Civil Engineering, The University of Sydney, Sydney, Darlington, NSW 2006, Australia
e-mail: omar.ismael@sydney.edu.au

M. O. Karkush and D. Choudhury (eds), *Modern Applications of Geotechnical Engineering and Construction*, Lecture Notes in Civil Engineering 112,
https://doi.org/10.1007/978-981-15-9399-4_2

1 Introduction

In the case of lateral loads, direct or passive, piles behave like transversely loaded beams and transfer loads to the surrounding soil by using the lateral resistance of the soil. Application of lateral loading on piles, a part or whole of the pile tries to move horizontally in the direction of loading which causes bending moment, rotation, and movement of the pile [1, 2]. The laterally loaded pile may be classified as an active pile or passive pile, regarding the method of transferring the loading direction between the pile and the surrounding soil [3–5]. An active pile is principally loaded at its top, with the lateral load being transferred to the soil, such as piles acting as foundations for transmission towers and offshore structures. A passive pile usually sustains lateral thrusts along its shaft arising from horizontal movement of the surrounding soil, such as piles in a moving slope [6]. Passive piles are extensively used next to the embankments and in moving slopes. In these systems, passive lateral pressure exerted to the pile by the moving soil causes displacements, moments and shear forces. The correct prediction of these values is a key element in the design, construction, and serviceability of the piles.

The influence of a passive pile on three-dimensional soil deformation around a laterally loaded pile and on the response of an active pile's in sandy soil has been investigated by conducting a series of model tests using a newly developed technique named Stereo-PIV [7]. A simple analytical method has been developed by Zhao et al. [8] and Zhang et al. [9] for simulating the effects of soil movement resulted from soil excavation on the behavior of pile groups. The lateral response of passive pile groups obtained from the proposed method has found to be well agreed with those obtained from centrifuge model tests. Furthermore, the behavior of piles subjected to lateral soil movement resulted from slopes has been investigated by conducting large-scale shear box [10]. The results of tests have been compared with those found in the literature to contribute to understanding the behavior of passive piles. Large geotechnical centrifuge model tests of two design schemes have been conducted to simulate the sheet-pile wharves with a load-relief platform in fine sand to investigate the distribution of lateral pile-soil pressure and to distinguish the pile's passive part from the active part [11]. The behavior of passive piles in fine-grained textured soil contaminated with two ratios of petroleum products (MFO) has been investigated under the effects of lateral soil movement [12, 13]. The obtained results of tests have shown an increase in the percentage of soil contamination has caused an increase in the impacts of embankment on the response of passive piles. A three-dimensional finite element model was established and the influence of pile spacing and pile-cap spacing on the displacement of soil around the pile has been analyzed. The results have shown that when the pile-cap spacing was less than 50 m, the soil settlement coefficient has almost changed linearly [14]. In the present study, the response of the existing flexible pile group of 2×1 to the lateral soil movement resulted from constructing a nearby embankment has been investigated.

2 Properties of the Materials

In this study, the soil, which was used, has been classified as (SP-SM) river sand according to the unified soil classification system (USCS). The geotechnical properties of the soil sample, which have been listed in Table 1, have been tested according to both the American (ASTM) standards and the British (BS) specifications [15, 16]. An aluminum pipe with a total length of 500 mm and a circular cross-section has been used to simulate the pile in this study by closing its both ends to prevent the soil to go inside the pile during the installation process. The mechanical properties of the aluminum pile have been listed in Table 2. A ratio of the pile length to its diameter (L/D) of 50 and an embedded depth (L_e) of 420 mm have been used in this study to ensure the flexible behavior of the pile group according to the flexibility factor (K_R) shown in Eq. 1 [17]. Where: E_p is the pile modulus of elasticity; I_p is the pile second moment of inertia; E_s is the soil secant modulus of elasticity and L_e is the pile embedded length.

$$K_R = \frac{E_p I_p}{E_s L e^4} < 10^{-5} \tag{1}$$

Four pairs of strain gauges, denoted as SG1 to SG4, with a gauge resistance of 120 ohms and a gauge factor of 2.12 ± 1% have been used to measure the bending strain along the model piles. The strain gauges have been fixed in two vertical lines with a 120 mm spacing, with the first pair at the soil surface, on both the near and the

Table 1 The geotechnical properties of the soil sample

Property	Value	Property	Value
Specific gravity (Gs)	2.67	Min dry unit weight (γ_{dmin}) [kN/m^3]	11.87
Coefficient of uniformity (Cu)	2.934	Max. dry unit weight (γ_{dmax}) [kN/m^3]	15.14
Coefficient of curvature (Cc)	1.188	Dry unit weight (γ_d) [kN/m^3] at Dr = 56%	13.5
Percentage of fines [%]	9.8	Friction angle (φ) [°] at Dr = 56%	35°
Percentage of sand [%]	90.2	Cohesion (c) [kPa]	9
Relative density (Dr) [%]	56	Confined elasticity modulus (E_{oed}) [kPa]	65770

Table 2 The mechanical properties of the model pile

Property	Value
Pile outer diameter (D)	10 [mm]
Thickness of pile wall	1 [mm]
Pile Length (L)	500 [mm]
Pile weight	42 [gm]
Density of aluminum	2.97 [gm/cm^3]
Pile modulus of elasticity (Ep)	69.871 [GPa]

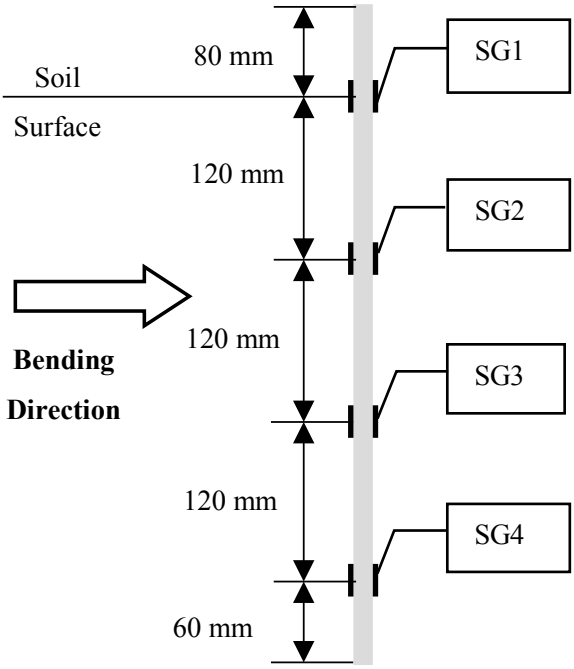

Fig. 1 Stain gauges arrangement along the pile in a half-bridge configuration

rear sides of the model pile with respect to the location of the embankment as shown in Fig. 1. Each pair of strain gages has been connected to a half-bridge configuration by Wheatstone bridge.

3 The Experimental Work

A steel box with a length of 800 mm, a width of 800 mm, and a height of 800 mm has been used to conduct the experimental work of this study. Sand has been poured in the box and densified to the required dry unit weight using the raining technique which required dropping the soil from a specific height. To calculate the required height, four dropping height ranged from 100 mm up to 400 mm with an increment of 100 mm have been adopted to study the effect of the dropping height on the dry unit weight of the soil as shown in Fig. 2. Based on Fig. 2 and to achieve a dry unit weight of 13.5 kN/m^3, a 240 mm dropping height has been adopted in this study. To maintain the dropping height, the dropping cone has been lifted a distance that equals the poured soil layer thickness.

A loading frame has been used to support the dropping cone system that used for the sand raining technique as well as a hydraulic jack of 10 tons capacity which is used for the piles installation process and the application of the embankment loads. Two (2 × 1) pile groups have been installed. One group, labeled as (LG) due to the

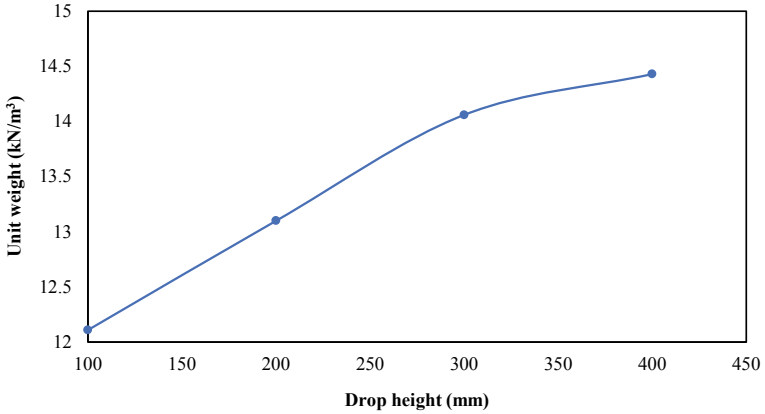

Fig. 2 The relation between the soil dry unit weight and the dropping height

application of axial loads, has been installed in the soil at a distance that exceeded 10 times the diameter of the pile from the steel box walls to ensure the elimination of any tip resistance effect [18]. While to ensure the elimination of rigid boundary effects [19], the other group, labeled as (UG) for the unloaded group, has been installed in the soil at a distance that exceeded 15 times the diameter of the pile from the loaded group (LG). Four dial gauges, two for each group, have been installed, one at the soil surface and the other one at the pile cap, to measure the horizontal displacement of each group. Surcharge loads of 10, 20, 30, 40, 50, and 60 kPa have been used to simulate the embankment loads at distances of 2.5, 5, and 10 times the diameter of the pile. A load cell mounted at the end of the hydraulic shaft has been used to monitor the magnitude of the applied surcharge loads. Each applied surcharge load has been maintained for 2 min as recommended by the literature [20, 21]. At each surcharge load, the strain gages readings as well as the dial gauge readings have been recorded with time.

4 Analysis of the Experimental Data

The flexural stress (σ_z) at the strain gauge locations has been calculated based on the measured bending strain (ε_z) by applying the elastic stress–strain relationship. Then, the discrete bending moment (Mz) has been calculated based on the calculated flexural stress (σ_z) using Eq. 2.

$$M_z = \frac{2\sigma_z I_p}{D} = \frac{2E_p \varepsilon_z I_p}{D} \tag{2}$$

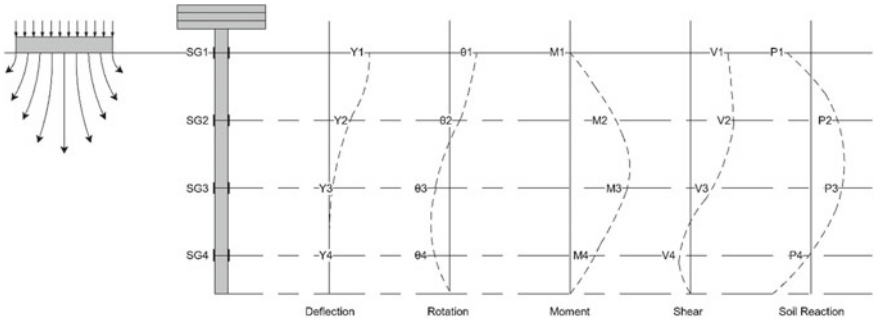

Fig. 3 Strain gages locations along the pile and patterns of calculated parameters

To convert the discrete bending moment to a continuous moment diagram along the pile, the literature has reported two approaches. One approach had been developed using the best-fit polynomial curve of the 4th to the 7th order. However, some drawbacks have been reported in the literature regarding this approach such as the inconsistency in selecting the best-fit curve as well as, in some cases, the sudden jump in the magnitude of the soil reaction at the pile tip [20, 22]. The other approach, [23–25], had been developed using the beam theory in which the responses of the pile and the reaction of the soil, see Fig. 3, could be derived from the bending moment.

Numerical integration following the trapezoidal rule has been adopted in this study to generate the profile of the bending moment along the pile. After this, the finite difference method [26], has been used to generate both the rotation and the deflection profiles along the pile as expressed in Eqs. 3 and 4. Where (θ_o and Y_o): are the rotation integration constant and the displacement integration constant, respectively, measured directly from the dial gauges at the head of the pile and Δ_z: is the distance between any two successive strain gauges as shown in Fig. 1a.

$$\theta_i = \sum_{i=0}^{n} \frac{M_i + M_{i+1}}{2} \nu z - \theta_o \tag{3}$$

$$Y_i = \sum_{i=0}^{n} \frac{\theta_i + \theta_{i+1}}{2} - \Delta z - n\Delta z\theta_o + Y_o \tag{4}$$

Finally, both the shear force profile (V_i) and the soil reaction profile (P_i) have been obtained by applying Eqs. 5 and 6, respectively, using five bending moments [27]. Two imaginary moments, labeled as M_5 and M_6 which assumed to be equal to M_4 and M_3, respectively, have been adopted to find the soil reaction (P4) based on the method described by Scott [28].

$$V_i = \frac{1}{2} \frac{M_{i-1} - M_{i+1}}{\nu z} \tag{5}$$

$$P_i = \frac{1}{7}\frac{2M_{i-2} - M_{i-1} - 2M_i - M_{i+1} + 2M_{i+2}}{\nu z^2} \quad (6)$$

5 Results and Discussion

The effects of constructed embankment adjacent to the pile group have been studied at three different distances from the edge of the model pile group equal to 2.5, 5 and 10 times the outer diameter of the model pile. Two loading conditions, axially loaded (LG) and unloaded (UG) pile groups, have been adopted in this study. The displacement of UG has been more than that of LG by 5% and 24% when the embankment constructed at distances of 5D and 10D, respectively, as shown in Fig. 4. While at a distance of 2.5D, LG has displaced more than UG at the soil surface by 21% due to the high pressure induced by the soil movement. Based on the results, the maximum displacement at the soil surface for the pile group has decreased by (60–64)% for LG and by (48–55)% for UG. The results obtained from the vertical loading tests and the tests of simulated embankment nearby axially loaded piles group are presented and discussed in this section.

The maximum rotation at the soil surface of LG increased by 415% with increasing the distance of the embankment from 2.5D to 5D because LG was rotated toward the embankment at distance 2.5D due to the high soil movement pressure as shown in Fig. 5. With increasing the distance from 5 to 10D, the maximum rotation at the soil surface decreased by 42% because the pressure of soil movement reduced as the distance increased. The rotation at the soil surface of UG decreased by (43–82)% as the distance increased from 2.5D to 10D as shown in Fig. 6. The UG group was not restrained with axial load and the rotation has decreased with increasing the distance due to the reduction in the pressure of soil movement.

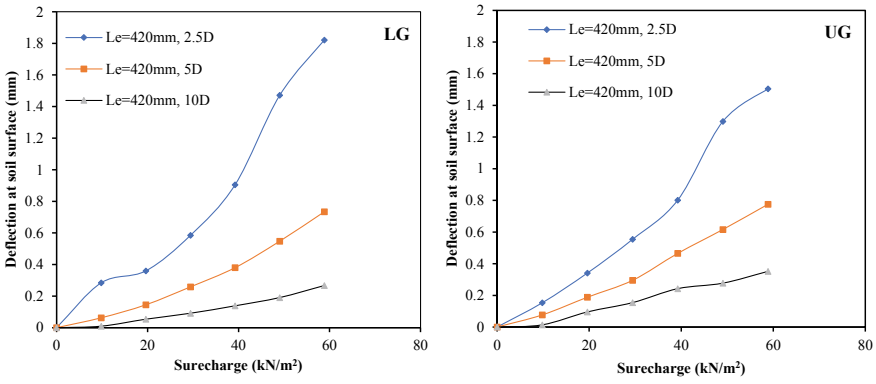

Fig. 4 Displacement of the pile group at the soil surface

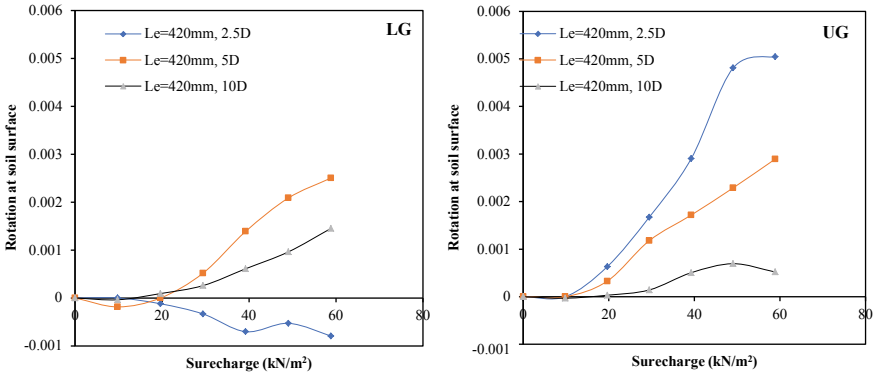

Fig. 5 Rotation of the pile group at the soil surface

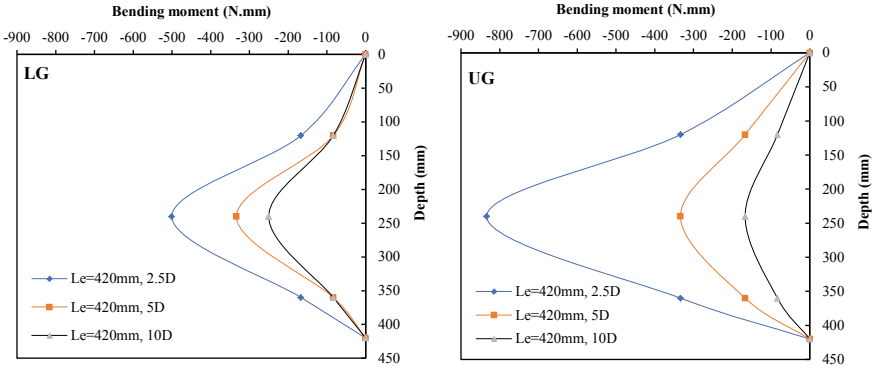

Fig. 6 Bending moment profiles of the pile group

The maximum moment is negative because the piles in the groups had bent under the reaction of the soil behind the piles as shown in Fig. 6. The maximum moment has decreased by (25–33)% for LG and by (50–60)% for UG with increasing the distance from 2.5D to 10D due to the long-embedded length of piles. The applied axial load has increased the stiffness of the pile group which in turn has reduced the maximum bending moment at high soil movement by 40% for LG in comparison with UG when the embankment at 2.5D. The effect of axial load in stiffening the piles group has decreased with increasing the distance. For 5D, the maximum moment in LG and UG is almost the same. While at a 10D distance, the maximum bending moment of LG has found to be increased to 50% when compared to UG.

The maximum deflection has decreased by (72–154)% in LG and by (47–61)% in UG when the distance increased from 2.5D to 10D, respectively, as shown in Fig. 7. The maximum deflection of LG is located at the piles tip when the embankment constructed at distance 2.5D due to the high soil movement and application of axial load which in turn has caused rotation toward the embankment. The maximum

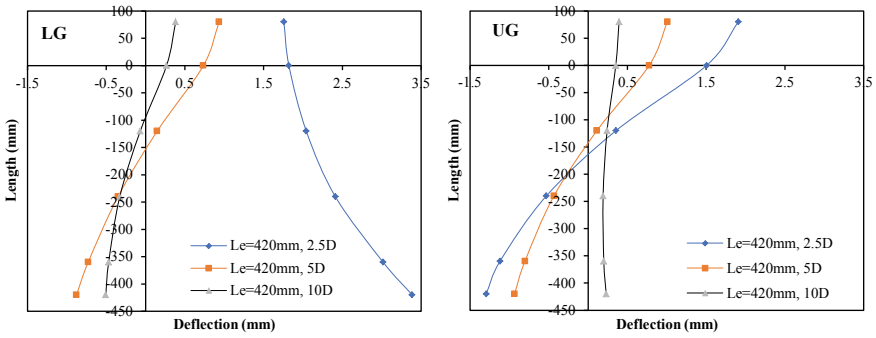

Fig. 7 Deflection profiles of the pile group

deflection of LG (at piles tips) has found to be more than that of UG (at piles heads) by 78% when the embankment constructed at a distance of 2.5D because LG has rotated toward the embankment due to the high soil movement and by 229% at distance 10D. While the maximum deflection of UG has found to be more than that of LG (at piles heads) by 7% when the embankment constructed at a distance of 5D.

The maximum rotation of LG is more than that of UG by 209% as shown in Fig. 8 when the embankment at 2.5D and 10D. While, the maximum rotation of UG is more than that of LG by 13% at 5D. The maximum rotation has increased by 146% then has decreased by 42% in LG, while it has decreased by 43% and 146% in UG with increasing the distance from 2.5D to 5D and from 5 to 10D, respectively. The maximum shear force has decreased by (25–33)% in LG and by (50–60)% in UG as the distance has increased from 2.5D to 10D, respectively, as shown in Fig. 9. This reduction has found to be related to the reduction in the bending moment for both LG and UG as described earlier.

The maximum soil reaction of negative sign has been defined as soil movement, while the soil reaction of positive sign has been defined as soil reaction. The soil reaction has decreased with increasing the distance between the edge of the pile

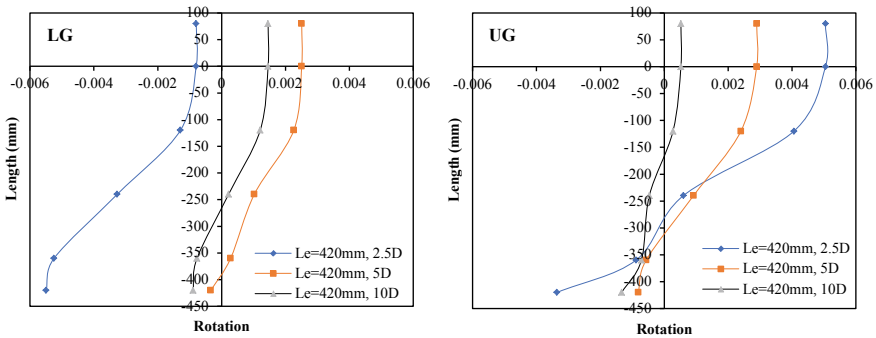

Fig. 8 Rotation profiles of the pile group

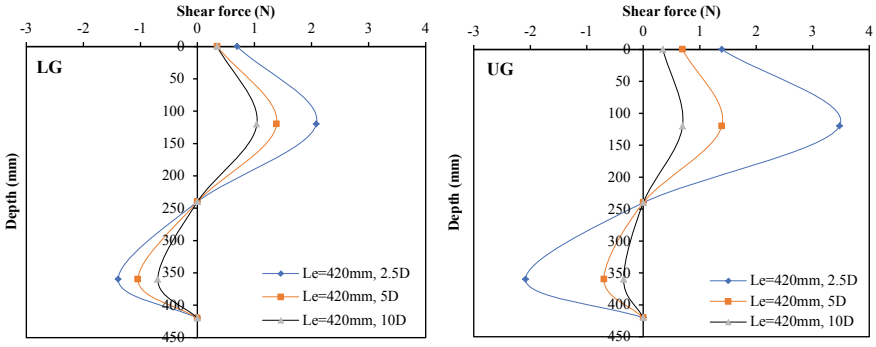

Fig. 9 Shear force profiles of the pile group

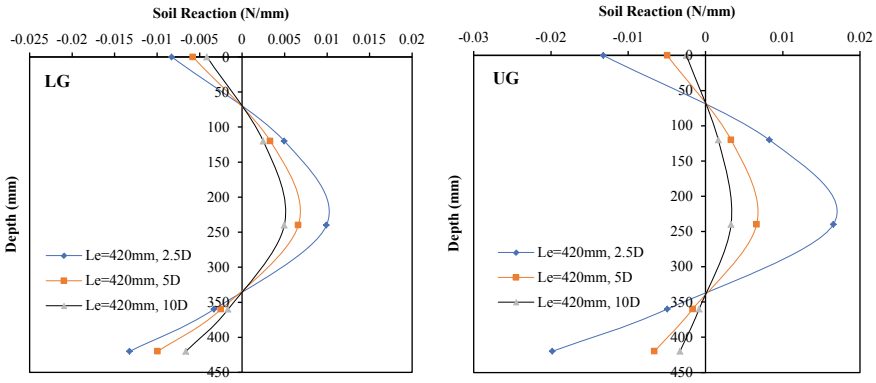

Fig. 10 Soil reaction profiles of the pile group

group and the embankment due to the reduction of soil movement pressure as shown in Fig. 10. The maximum soil reaction has decreased by 33% and 25% in LG and by 60% and 50% in UG with increasing the distance from 2.5D to 5D and from 5 to 10D, respectively.

6 Conclusions

The construction of a nearby embankment or surcharge load will affect the performance of the existing pile foundation. Based on the results obtained from the present study, the following conclusions can be drawn out:

- The application of axial load decreased the displacement at the soil surface, where UG displaced more than LG at 5D and 10D, respectively. However, at 2.5D, LG has displaced more than UG.

- The maximum deflection of LG has found to be more than that of UG when the embankment constructed at distances of 2.5D and 10D, respectively. However, the maximum deflection of UG has found to be more than that of LG by 7% at 5D.
- The maximum shear force in UG is more than that in LG by 40% when the embankment at distances of 2.5D and 5D. At 10D, the maximum shear force in LG is more than that in UG by 50%.
- The maximum displacement at the soil surface has decreased with increasing the distance between the pile and the edge of embankment from 2.5D to 10D in LG and UG, respectively.
- The soil reaction has decreased with increasing the distance between the edge of the piles and the embankment due to the reduction of soil movement pressure.

References

1. Salgado R, Basu D, Prezzi M (2008) Analysis of laterally loaded piles in multilayered soil deposits. Joint Transportation Research Program, Paper 330
2. Fleming WGK (1992) A new method for single pile settlement for prediction and analysis. Geotechnique 42(3):411–425
3. Ercan A (2010) Behaviour of pile groups under lateral loads. M.Sc. Thesis, Civil Engineering Department, Middle East Technical University
4. Fleming WGK, Weltman AJ, Randolph MF, Elson WK (2008) Piling engineering. Taylor and Francis, London and New York
5. Beer D (1977) Piles Subjected to static lateral loads. Doctoral dissertation, Gent Royal Institute for Soil Mechanics
6. Qin H (20101) Response of pile foundations due to lateral force and soil movements. Ph.D. Thesis, Griffith University, School of Engineering
7. Yuan B, Chen R, Teng J, Peng T, Feng Z (2014) Effect of passive pile on 3D ground deformation and on active pile response. Sci World J
8. Zhao M, Liu D, Zhang L, Jiang C (2008) 3D finite element analysis on pile-soil interaction of passive pile group. J Cent South Univ Technol 15:75–80
9. Zhang CR, Huang MS, Liang FY (2009) Lateral responses of piles due to excavation-induced soil movements. In: Ng, Huang, Liu (eds) Geotechnical aspects of underground construction in soft ground 2009. Taylor & Francis Group, London
10. Ersoy CO, Yildirim S (2014) Experimental investigation of piles behavior subjected to lateral soil movement. Teknik Dergi 25(4):6867–6888
11. Ren GF, Xu GM, Gu XW, Cai ZY, Shi BX, Chen AZ (2018) Centrifuge modelling for lateral pile-soil pressure on passive part of pile group with platform. In: Physical modelling in geotechnics vol 1. CRC Press, pp 583–587
12. Karkush MO, Kareem ZA (2018) Investigation the impacts of fuel oil contamination on the behaviour of passive piles group in clayey soils. Eur J Environ Civil Eng 1–17
13. Karkush MO, Kareem ZA (2019) Behavior of passive pile foundation in clayey soil contaminated with fuel oil. KSCE J Civil Eng 23(1):110–119
14. Liu N, Yu J, Gong X, Chen Y (2018) Analysis of soil movement around a loaded pile induced by deep excavation. In: IOP conference series: earth and environmental science, vol 189(3). IOP Publishing, p 032053
15. American Society for Testing and Materials (2003) Annual book of ASTM standards: soil and rock. ASTM, Philadelphia, PA

16. British Standards BS 1377 (1976) Methods of testing for civil engineering purpose. British Standards Institution, London
17. Poulos HG, Davies EH (1980) Pile foundation analysis and design. Wiley, New York, NY
18. Bolton MD, Gui MW, Garnerier J, Corte JF, Bagge G, Laue J, Renzi R (1999) Centrifuge cone penetration tests in sand. ASCE 49(4):543–552
19. Kishida H (1967) The ultimate bearing capacity of pipe piles in sand. In: Proceedings of the 3rd asian regional conference of soil mechanics and foundation engineering, vol 1. pp 196–199
20. Springman SM (1989) Lateral loading on piles due to simulated embankment construction. Unpublished doctoral dissertation, Cambridge University, England
21. Bransby MF, Springman SM (1997) Centrifuge modeling of pile groups adjacent to surcharge loads. Soils Found Jpn Geotechn Soc 37(2):39–49
22. Stewart DP (1992) Lateral loading of piled bridge abutments due to embankment construction. Unpublished doctoral dissertation, University of Western Australia, Australia
23. Ismael OK, Han J (2015) Model tests of laterally loaded piles under a horizontally scoured condition. In: IFCEE 2015, pp 802–808
24. Ismael OK (2014) Evaluating the behavior of laterally loaded piles under a scoured condition by model tests. Master Thesis, University of Kansas
25. Muthukkumaran K (2013) Effect of slope and loading direction on laterally loaded piles in cohesionless soil. Int J Geomech 14(1):1–7
26. Chen F, Yang M (2005) Numerical analysis of piles influenced by lateral soil movement due to surcharge loads. Chin J Geotechn Eng 27(11):1286–1291
27. Levachev SN, Fedorovsky VG, Kurillo SV, Kolesnikov YM (2002) Piles in hydrotechnical engineering. Taylor and Francis
28. Scott RF (1981) Foundation analysis. Prentice-Hall, Englewood Cliffs, NJ

Evaluating End-Bearing and Skin-Friction Resistance of Test Pipe Pile in Sand Soil

Wissam H. S. Al-Soudani and Bushra S. Albusoda

Abstract The present study explained a technique to separate the bearing capacity of pipe pile into skin friction and end bearing by adopting an experimental testing program. Close-end and open-end test pipe pile have considered. The technique depends on the manufactured movable steel container for a mini circular load cell (Dm = 15 mm) to measure the end bearing resistance of the pipe pile with a diameter 40 mm. The competence of this technique was studied by manufacturing and modeling the two pipe piles types with different lengths according to ratios of the lengths to a diameter that was considered in this study (L/D = 15 and L/D = 20). The model piles were tested in loose dry sand. The soil plugging phenomenon and the Incremental Filing Ratio IFR were studied. The complete setup is manufactured for installing and loading the piles at a constant rate of penetration. The obtained results show that the skin-friction less than the end bearing resistance for all pipe pile tests. The distribution of skin-friction tends to become constant below the critical depth of the pile into the sand container. Also, the distribution of skin friction will depend on the lengths to diameter ratios. Also, the end bearing resistance is more than the exterior shaft friction resistance for both pile length 600 and 800 mm.

Keywords Open-ended (OE) pipe pile · Closed-ended (CE) pipe pile · End-bearing capacity · Skin friction capacity · Plug capacity

1 Introduction

The foundation of the building structures in the offshore and land are still nowadays used the deep foundation type hollow pipe pile OE and CE. The OE is classified as a low displacement pile and has a low effect on the surrounded soil during installation.

W. H. S. Al-Soudani (✉) · B. S. Albusoda
Department of Civil Engineering, University of Baghdad, Baghdad, Iraq
e-mail: wissam.hadi@gmail.com

B. S. Albusoda
e-mail: albusoda@yahoo.com

M. O. Karkush and D. Choudhury (eds), *Modern Applications of Geotechnical Engineering and Construction*, Lecture Notes in Civil Engineering 112,
https://doi.org/10.1007/978-981-15-9399-4_3

During the pile driving into the ground, the soil will move up inside the pile and formed a soil plug. The entrance of soil will continue until the inner soil cylinder mode develops sufficient resistance to prevent further soil intrusion. If the stresses in the inner soil are sufficient to resist and prevent further soil intrusion inside the pipe pile, the pile will act as a full plugged CE. Thus, if the shear resistance developed along the length of the column of the restricted soil more than the end bearing capacity at the base of the soil plug, the pile will fail in the plugged mode. On the other hand, the pipe pile will fail in unplugged mode when the shear failure occurs between the soil plug and the pile shaft. The analytical methods and some field tests like chamber tests are still considered as design criteria for OE, suggested from [1–4].

American Petroleum Institute [5] used to evaluate the bearing capacity for OE for the different modes of the OE like unplugged and full plugged mode. The OE when installed in sands behave in partially plugged mode. Stefanoff and Boshinov [6], referred possibility the soil plug can be modeling by one-dimensional analysis, by taking a series of horizontal thin discs to simulate the length of the soil plug and these discs are connected by equilibrium condition represented by a force applied to each disc in final these forces used to measure the plug capacity of the OE. Fattah and Al-Soudani [7] explained that when soil entering the pipe pile during installation, the pile can be fully plugged or partially plugged where the external skin friction and internal skin friction will be mobilized during driving the pile into the ground [8]. Tested a special type of full-scale OE in the field (northern Indiana), that is represented by the double-walled OE that is constituted of two hollow pipes with different diameters as shown in Fig. 1a. Figure 1b explained the curve of separation total pile capacity to major components (shaft friction capacity and end bearing capacity) during the applied loading test. The figure explained a constant behavior resistance of the shaft

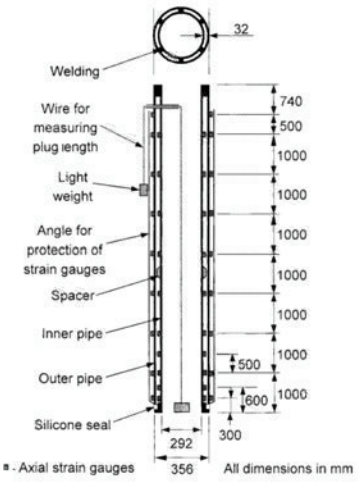

Schematic double-walled (OE)

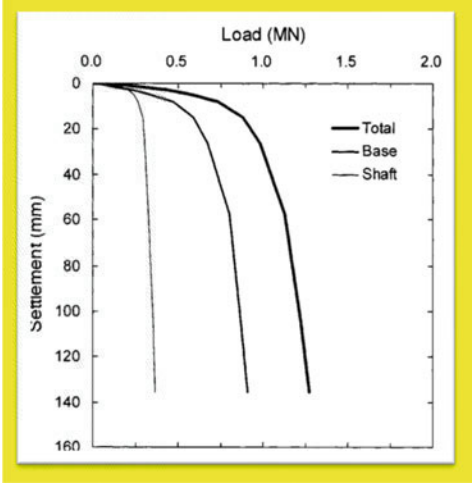

Separation total pile capacity to major components

Fig. 1 Schematic and Load settlement curves of full-scale test pile by [9]

friction capacity at the end of the loading test, while the end bearing capacity can be considered at the settlement of 35.6 mm, corresponding to 10% of the pile diameter.

2 Experimental Work

Four steel traditional pipe piles (open-ended and closed-ended) are used for testing (static axial compression loading) within loose sandy soil.

Soil Properties. The soil used in the study was clean sand from Karbala city, with poorly graded, the properties of the sand (physical and mechanical) were evaluated according to the ASTM standards, that explained in Table 1.

The loose density of the soil sample was prepared by letting the sands falling from a constant height like a raining by depending on the raining method. And to decreases the speed of the falling soil particles, by sand diffuser that includes sieves No. 10 to get sand with a relative density of (25%).

Model Setup Formulation. The loading system is manufactured to simulate that of the field-test, it comprises Steel Structure of frame model; steel tank container; steel moveable girder loading system; steel moveable axial loading system; compression load cell type(s); mechanical jack; gearbox; weighing indicator; speed regulator; raining apparatus; dial gauge indicator; pile driving installation system and reading board. The moveable loading system allows testing the pile models at any location in the steel container and can apply different types of loading in a different direction, as shown in Fig. 2.

Table 1 Properties of the sand (physical and mechanical) considered are in the study

Index	Value	Standard
Coefficient of uniformity (Cu)	2.63	–
Coefficient of curvature (Cc)	1.42	–
Grain size analysis	–	ASTM D 422-2007
Specific gravity (Gs)	2.63	ASTM D 854-2014
D10 (mm)	0.16	–
D30 (mm)	0.28	–
D50 (mm)	0.35	–
Soil classification (USCS)	SP	–
Maximum dry unit weight (kN/m^3)	17.4	ASTM D 4253-2014
Minimum dry unit weight (kN/m^3)	15.46	ASTM D 4254-2000
Maximum void ratio	0.667	–
Minimum void ratio	0.482	–

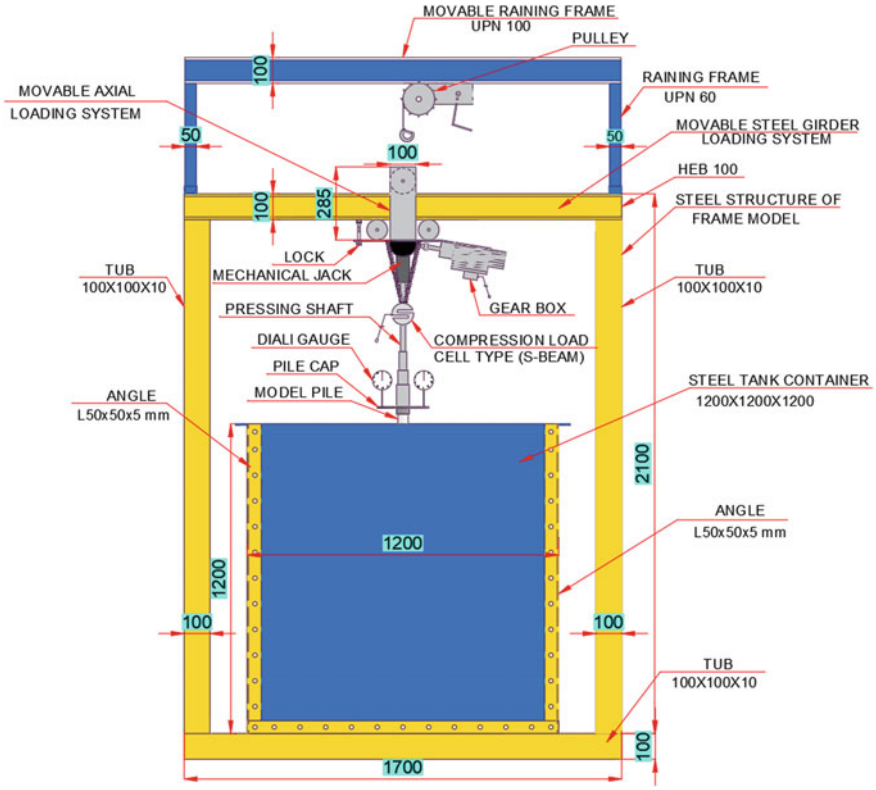

Fig. 2 Complete set up for model pile testing

Model Pile. Four models of the pile (steel pipe) were used and investigated in the study. These piles executed in the loose sand by hammering (free drop hammer). The piles model was illustrated by a diagram in Fig. 3. The lengths of the piles model (600 and 800 mm) were considered in the experimental testing program, with an outside diameter of 40 mm and thickness of the pile wall (2 mm). These models have named as Open-End Pipe Piles (OE) and Closed-End Pipe Piles (CE). An OE piles commonly was behaved in a partially plugged mode when driven into sands. Then the total capacity of OE composed of the annular load capacity, plug load capacity, and shaft load capacity.

3 Testing Program

Four models (OE and CE) tests have executed in dry sand soil samples, with loose relative densities. These piles were driven by a drop hammer (40 N) with a free-drop from a height of 200 mm. When pile driving, the pile penetration depth, and soil plug

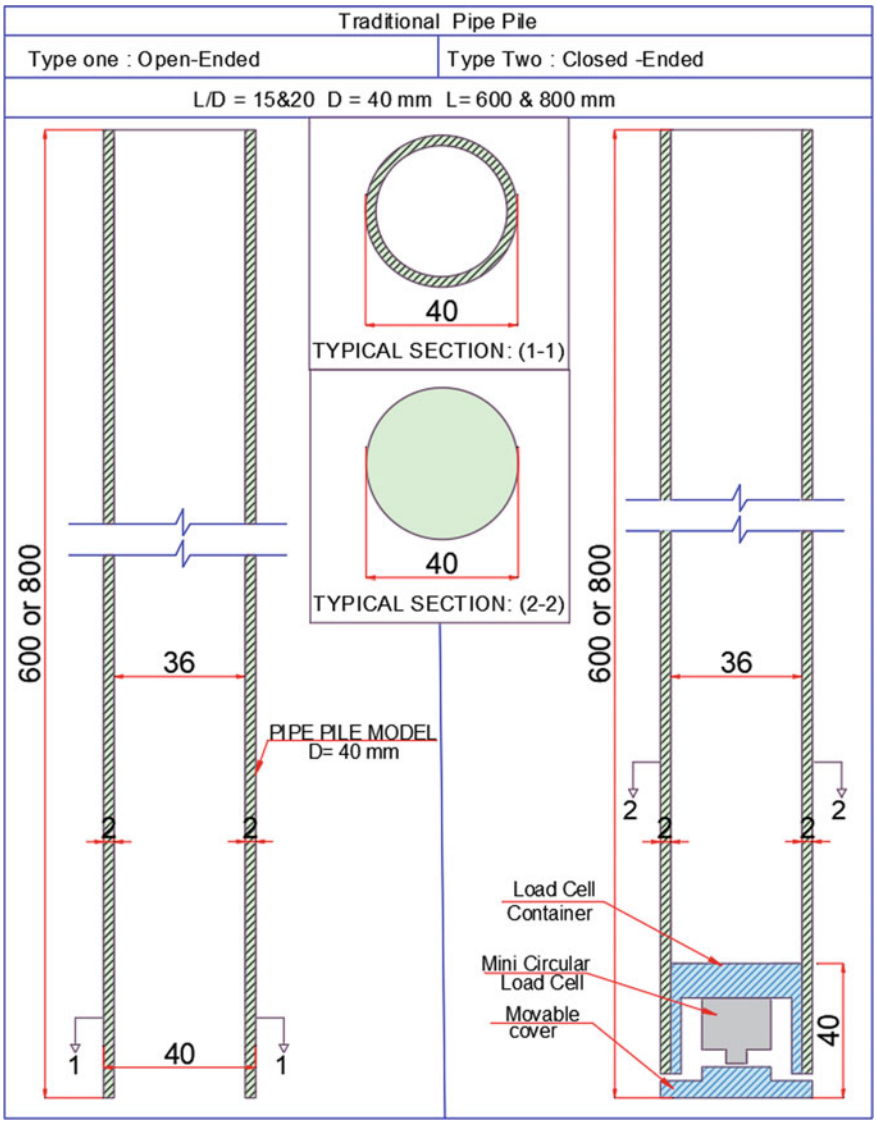

Fig. 3 Traditional OE and CE were piles used in the study

length were measured for every five blows intervals to calculate the incremental filling ratio (IFR). The variation in the soil plug length when pile driving was measured using a ruler entered inside the pipe pile. Axial static load compression has performed at a CRP by using a mechanical jack. The total applied load on the pile has evaluated by a load cell, and the settlement of the pile has evaluated by dial gages. The load tests have continued until the plunging failure.

Separation of the shaft friction resistance and the end bearing resistance from total pile capacity. To parting the total pile load capacity into shaft friction and the end bearing resistance, an instrumented circular steel container includes a mini-load cell inside it was used to measure the end bearing resistance of the closed-end pipe pile model, as shown in Figs. 4 and 5.

Steel Circular Container for Circular Mini Load Cell. A steel circular container was manufactured, to put a mini circular cell inside it, with a diameter (39 mm), and height 40 mm. The steel circular container has locked by the cover. It contains an apex aciculate in the center with a height of 2 mm to connect with the apex of the load cell. The cover is movable in the vertical direction, through a vertical interval distance of (1 mm) between the apex as shown in Figs. 4 and 5. The load cell has stabilized inside the steel container.

Distribution of the Resistance Forces of Soil along the Length of the Traditional Pipe Piles. Figure 6 explains the distribution of the resistance forces of soil along the external piles' body. Three types of traditional pipe pile have considered. The first type represents the distribution of the resistance forces for an unplugged pipe pile, whereas the total capacity of the pile includes the exterior and interior shaft friction forces along the external piles' body. The end-bearing resistance forces that represented only under the annular wall of the pipe pile. The second type for open-end pipe pile with a plugged mode in which the total resistance force is similar to the behavior of the third type of the CE, that the total resistance of these piles includes the exterior shaft friction forces along the external piles' body and the end-bearing resistance for a total area end bearing.

Length of the Soil Plug (Lp) and Measurements the Incremental Filling Ratio (IFR) for Traditional OE Pipe Pile. The (Lp) as shown in Fig. 7 and the (IFR) have measured for two piles of the traditional open-end pipe piles with different lengths, as shown in Fig. 8.

Definition of failure load: According to [8], that explains two criteria are commonly used to define the failure axial pile load capacity under static compression load.

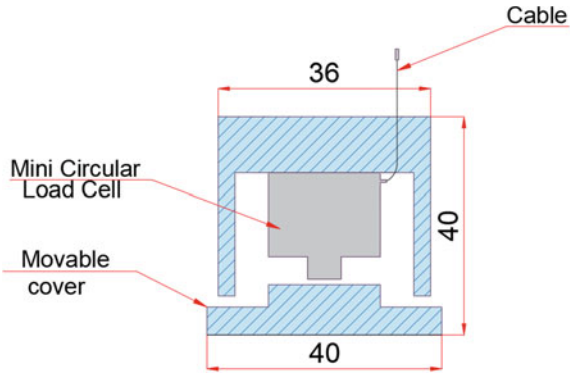

Fig. 4 Details of the steel container of load cells

Fig. 5 Types of the steel container of load cells to measure end bearing resistance

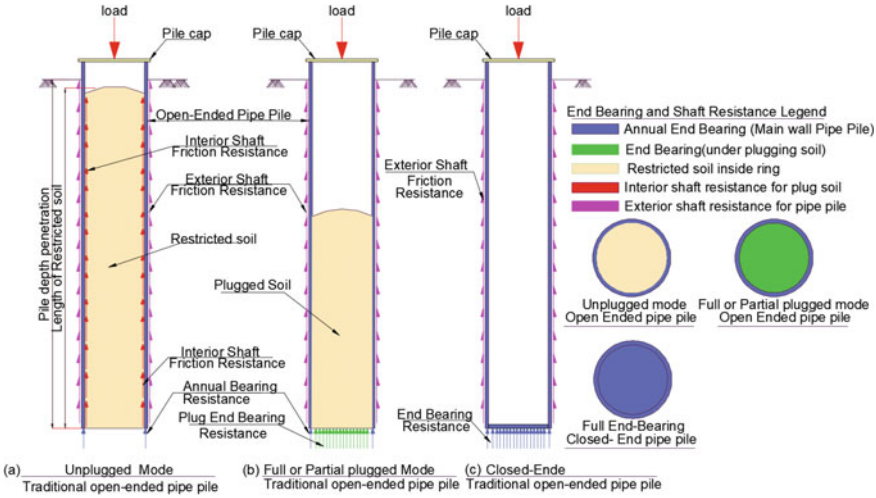

Fig. 6 Distribution of the resistance forces of soil along the external piles' body

Ultimate capacity (plunging failure). The failure load represents the load at which settlement continues indefinitely, as shown in Fig. 8. At field testing, pile load testing cannot use sufficient loads to reach this type of failure. Plunging failure has been reached when using a constant rate of penetration test (CRP).

Deformation controlled capacity. This concept is based on the failure load. It is the load at which the settlement of pile reaches 10% of the diameter of the pile

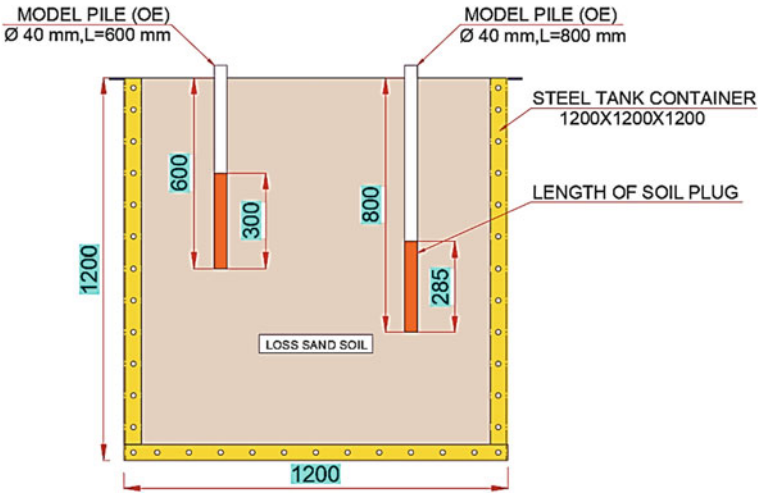

Fig. 7 Length of soil plug for traditional open-end pipe pile

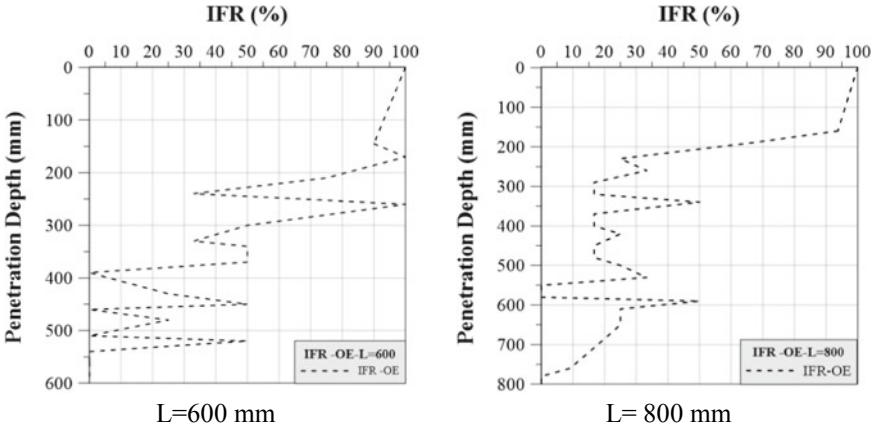

Fig. 8 Incremental filling ratio (IFR) for traditional open-end pipe pile (OE)

base, as shown in Fig. 9. In the present study, the failure load (ultimate capacity) has considered as the load that causes plunging failure, due to the type of loading test is the constant rate of penetration (CRP).

Interpretation of ultimate pile load capacity (failure load). A 30 mm displacement of the pile into the sand container has considered ensuring the mobilization of the end bearing and pile reaches the failure condition. Fleming et al. [10] showed that the true ultimate capacity of the tested pile can be evaluated when the shaft friction essentially is fully mobilized. It is recommended to mobilize the conceivable rate of end bearing. This means that for good analysis, it needs a settlement over around

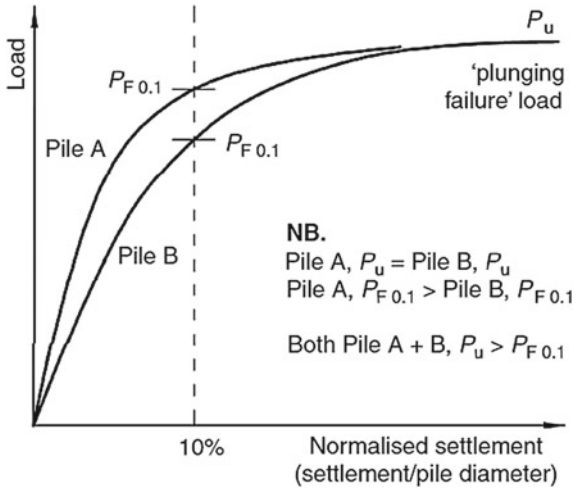

Fig. 9 Definitions of pile failure

25 mm for the tested pile. The [11] and [8] defined the load at failure as the load at which the rate of settlements continues lowering without further increment of the load.

Presentation Result for Traditional Pipe Pile (Open-End and Closed-End). Four traditional pipe piles with two types, open-end (OE) and closed-end (CE), with different lengths to the diameter ratios (L/D = 15 and 20). Figure 10 presents the curves of the relation between the applied load and pile head settlement for traditional OE with partial plugged and CE. It can be noticed that all curves of the relation between applied load and pile head settlement exhibit punching shear failure.

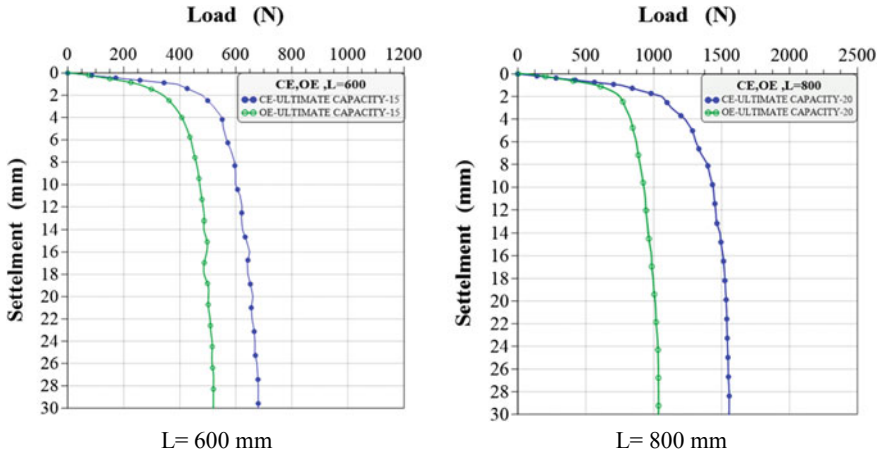

L= 600 mm L= 800 mm

Fig. 10 Curves of the relation between applied load and pile head settlement (OE and CE) performed in loose sand